Hindawi Publishing Corporation
Shock and Vibration
Volume 2014, Article ID 937967, 8 pages
http://dx.doi.org/10.1155/2014/937967

*Research Article*

# Regular and Chaotic Dynamics of Flexible Plates

**J. Awrejcewicz,[1,2] E. Yu. Krylova,[3] I.V. Papkova,[3] and V. A. Krysko[3]**

[1] *Department of Automation, Biomechanics and Mechatronics, Lodz University of Technology, 1/15 Stefanowski Street, 90-924 Lodz, Poland*
[2] *Department of Vehicles, Warsaw University of Technology, 84 Narbutta Street, 02-524 Warszawa, Poland*
[3] *Department of Mathematics and Modeling, Saratov State Technical University, Russian Federation, Politehnicheskaya 77, Saratov 410054, Russia*

Correspondence should be addressed to J. Awrejcewicz; awrejcew@p.lodz.pl

Received 27 June 2013; Accepted 19 December 2013; Published 1 July 2014

Academic Editor: Nuno Maia



Nonlinear dynamics of flexible rectangular plates subjected to the action of longitudinal and time periodic load distributed on the plate perimeter is investigated. Applying both the classical Fourier and wavelet analysis we illustrate three different Feigenbaum type scenarios of transition from a regular to chaotic dynamics. We show that the system vibrations change with respect not only to the change of control parameters, but also to all fixed parameters (system dynamics changes when the independent variable, time, increases). In addition, we show that chaotic dynamics may appear also after the second Hopf bifurcation. Curves of equal deflections (isoclines) lose their previous symmetry while transiting into chaotic vibrations.

## 1. Introduction

Plates as thin-walled structural members are widely applied in various branches of industry, civil engineering, and factories producing measurement devices. Nowadays modeling procedures and dynamics investigation are very complex and require confirmation of the reliability and validity of results obtained. One of the ways to get more reliable results is to develop more adequate mathematical models for studying of continuous mechanical systems. The developed models are expected to exhibit important nonlinear effects including the influence of geometric nonlinearity as well as external load properties on the system chaotic dynamics. Nonlinear vibrations of real continuous systems can be very complicated. Majority of the signals (time series) obtained through the numerical experiments are nonstationary ones; that is, they strongly change in time. Therefore, in spite of the traditional approaches, including FFT (fast Fourier transform), additional methods are highly required. We illustrate the advantages of application of wavelet transforms for detecting and monitoring local properties of the analyzed time series (signals). The latter approach allows for the detection of local signal properties.

It is clear that modeling of plates/shells dynamics has a long history, and there are numerous papers and monographs dedicated to this research area. We refer only to a few of them more adequately fitting our research aims and the used methods. The existence of heteroclinic loops, Smale horseshoes, chaotic dynamics, and symmetry breaking phenomena of a nearly squared plate are discussed in [1, 2].

Chaotic vibrations of a shallow cylindrical shell subjected to harmonic lateral excitation are studied via the Galerkin approach allowing for a reduction of the initial infinite problem to that of finite dimension (multiple degrees of freedom) by Yamaguchi and Nagai [3]. Luo derived analytical conditions for the chaotic dynamics of axially travelling thin plates using the incremental energy approach. Poincaré mapping sections are used for monitoring of chaotic motions in primary resonant and homoclinic separation zones [4]. Nonlinear dynamics of bimetallic circular plates under time-varying temperature load is studied by Wang [5], where the onset of chaos, transient chaos, period doubling, and reversed period doubling scenario, among other items, are illustrated and discussed. A transition from regular to wave turbulence regime exhibited by thin plates harmonically loaded is illustrated and discussed in references [6, 7].

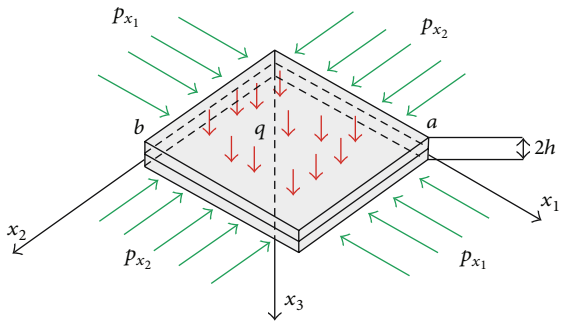


FIGURE 1: Plate computational scheme.

Transitions into the system with finite (many) degrees of freedom chaotic dynamics are reported in a series of references [8–12]. The advantages of wavelet-oriented analysis of nonlinear vibrations of continuous mechanical systems are described in [13]. Although we aim here at numerical investigations, it should be noted that there is a possibility to apply the method of an artificial perturbation parameter to study nonlinear plate vibrations [14].

## 2. Differential and Difference Governing Equations

The mathematical model of vibrations of a flexible rectangular plate (shown in Figure 1) with constant stiffness subjected to the action of time periodic longitudinal load distributed along the plate perimeter is constructed on the basis of the kinematic Kirchhoff-Love approach taking into account the nonlinear dependence between deformations and displacements. We introduce small initial static load in the initial time interval $t \in [0; 1]$. In rectangular coordinates the system of 3D space is presented in the following form:

$$\Omega = \{x_1, x_2, x_3 \mid (x_1, x_2) \in [0; a] \times [0; b], \quad x_3 \in [-h; h]\}, \quad 0 \le t < \infty. \tag{1}$$

We apply the following nondimensional PDEs governing dynamics of our plate:

$$\begin{aligned} &\frac{1}{12(1-\mu^2)}\left(\nabla_\lambda{}^4 w\right) - L(w, F) + \frac{\partial^2 w}{\partial t^2} \\ &\quad + \varepsilon\frac{\partial w}{\partial t} - q(x_1, x_2, t) = 0, \\ &\nabla_\lambda{}^4 F + \frac{1}{2}L(w, w) = 0, \end{aligned} \tag{2}$$

where

$$\begin{aligned} \nabla_\lambda{}^4 &= \frac{1}{\lambda^2}\frac{\partial^4}{\partial x_1{}^4} + \lambda^2\frac{\partial^4}{\partial x_2{}^4} + 2\frac{\partial^4}{\partial x_1{}^2 \partial x_2{}^2}, \\ L(w, F) &= \frac{\partial^2 w}{\partial x_1{}^2}\frac{\partial^2 F}{\partial x_2{}^2} + \frac{\partial^2 w}{\partial x_2{}^2}\frac{\partial^2 F}{\partial x_1{}^2} - 2\frac{\partial^2 w}{\partial x_1 \partial x_2}\frac{\partial^2 F}{\partial x_1 \partial x_2} \end{aligned} \tag{3}$$

are the nonlinear operators and $w$ and $F$ are the functions describing deflection and stresses, respectively.

Simple boundary conditions are attached to (2):

$$\begin{aligned} &w = 0; \quad \frac{\partial^2 w}{\partial x_1{}^2} = 0; \quad F = 0; \quad \frac{\partial^2 F}{\partial x_1{}^2} = p_{x_2} \\ &\qquad \text{for } x_1 = 0; 1; \\ &w = 0; \quad \frac{\partial^2 w}{\partial x_2{}^2} = 0; \quad F = 0; \quad \frac{\partial^2 F}{\partial x_2{}^2} = p_{x_1} \\ &\qquad \text{for } x_2 = 0; 1, \end{aligned} \tag{4}$$

and the following initial conditions are applied:

$$w(x_1, x_2)\big|_{t=0} = 0, \qquad \left.\frac{\partial w}{\partial t}\right|_{t=0} = 0. \tag{5}$$

Equations (2)–(5) are reduced to the nondimensional form using the following nondimensional parameters: $\lambda = a/b$; $x_1 = a\overline{x}_1$, $x_2 = b\overline{x}_2$ are the nondimensional parameters regarding $x_1$ and $x_2$, respectively; $w = 2h\overline{w}$ is the deflection; $F = E(2h)^3\overline{F}$ is the stress function; $t = t_0\overline{t}$ is time; $q = (E(2h)^4/a^2b^2)\overline{q}$ is the external pressure; $\varepsilon = (2h)\overline{\varepsilon}$ is the damping coefficient; and $p = E(2h)^3\overline{p}$ is the external longitudinal load. Bars over the nondimensional quantities are already omitted in the governing equations. Additionally, $a$ and $b$ are the plate dimensions regarding $x_1$ and $x_2$, respectively; $\mu$ is Poisson's coefficient.

In "Mechanics" the degrees of freedom are understood as the set of independent coordinates, which together with their time derivatives describe the mechanical system state [15]. The choice of the number of degrees of freedom of the studied system depends on a real system behavior. Since in majority of the real world mechanical systems the constraints are not absolutely stiff, the real number of degrees of freedom equals a triple number of the atoms associated with the system material volume. In the case of the continuous system we deal with the infinite number of degrees of freedom. In many cases in the engineering practice, approximations are used which enable a drastic decrease of the degrees of freedom, not exceeding six. It is clear that this drastic approximation may lead either directly to erroneous results, that is decrease of modes number.

Dynamical systems may exhibit four different types of stationary regimes: equilibrium, periodic, quasiperiodic, and chaotic dynamics. The mentioned regimes are associated with attractors in the form of a stable equilibrium point, limit cycle, and quasiperiodic attractor (multiple dimensional torus) as well as strange chaotic attractor, respectively. Recall that the quasiperiodic and chaotic attractors may appear in dynamical systems with the space phase dimension being larger than three.

In order to reduce a continuous system to the system with lumped parameters regarding spatial variables $x_1$ and $x_2$, the FDM (finite difference method) with approximation of $O(h^2)$ is applied, allowing us to consider flexible rectangular plates

Table 1: Plate bifurcations.

| Points | | 1st bifurcation | 2nd bifurcation | 3rd bifurcation | 4th bifurcation | Difference between theoretical and computed value in % |
|---|---|---|---|---|---|---|
| 12 | $S_{0,n}$ | 13.675 | 13.735 | 13.7465 | 13.74894 | |
| | $d_n$ | | 5.217391 | 4.713115 | | 0.22006 |
| 14 | $S_{0,n}$ | 13.44 | 13.49 | 13.500078125 | 13.502232 | |
| | $d_n$ | | 4.96124... | 4.67906679... | ... | 0.21847 |
| 16 | $S_{0,n}$ | 13.27 | 13.323 | 13.334 | 13.33635 | |
| | $d_n$ | | 4.818182 | 4.673519 | | 0.21821 |

as the mechanical systems with infinite degrees of freedom. The application of FDM to the continuous system yields the following set of the difference-operator equations:

$$
\begin{aligned}
&-\frac{1}{12\left(1-\mu^2\right)}\left(\lambda^{-2}\Lambda_1^2 w_{ij}+2\Lambda_{12}^2 w_{ij}+\lambda^2\Lambda_2^2 w_{ij}\right)\\
&\quad-\Lambda_1 w_{ij}\cdot\Lambda_2 F_{ij}-\Lambda_2 w_{ij}\cdot\Lambda_1 F_{ij}+\Lambda_{12} w_{ij}\cdot\Lambda_{12} F_{ij}\\
&\quad+q_i=\left(w_{tt}+\varepsilon w_t\right)_{i,j},\\
&\left(\lambda^{-2}\Lambda_1^2 F_{ij}+2\Lambda_{12}^2 F_{ij}+\lambda^2\Lambda_2^2 F_{ij}\right)\\
&\quad=-\Lambda_1 w_{ij}\cdot\Lambda_2 w_{ij}+\left(\Lambda_{12} w_{ij}\right)^2,
\end{aligned}
\tag{6}
$$

where

$$
\begin{aligned}
\Lambda_i y&=\frac{1}{h_i^2}\left[y\left(x_i-h_i\right)-2\cdot y\left(x_i\right)+y\left(x_i+h_i\right)\right],\\
&\qquad\qquad i=1,2,\\
\Lambda_{12} y&=\frac{1}{4h_1h_2}\left[y\left(x_1+h_1,x_2+h_2\right)+y\left(x_1-h_1,x_2-h_2\right)\right.\\
&\qquad\left.-\left(x_1+h_1,x_2-h_2\right)-\left(x_1-h_1,x_2+h_2\right)\right],\\
\Lambda_i^2 y&=\frac{1}{h_i^4}\left[y\left(x_i-2h_i\right)-4y\left(x_i-h_i\right)+6y\left(x_i\right)\right.\\
&\qquad\left.-4y\left(x_i+h_i\right)+y\left(x_i+2h_i\right)\right]\quad i=1,2,\\
\Lambda_{12}^2 y&=\frac{1}{h_1^2h_2^2}\left[y\left(x_1-h_1,x_2-h_2\right)-2y\left(x_1-h_1,x_2\right)\right.\\
&\qquad+y\left(x_1-h_1,x_2-h_2\right)-2\left(x_1,x_2-h_2\right)\\
&\qquad+4y\left(x_1,x_2\right)-2y\left(x_1,x_2+h_2\right)\\
&\qquad+y\left(x_1+h_1,x_2-h_2\right)\\
&\qquad\left.-2\left(x_1+h_1,x_2\right)+y\left(x_1+h_1,x_2+h_2\right)\right].
\end{aligned}
\tag{7}
$$

Equations (7) are supplemented with boundary conditions (4), which have the following difference representation (flexible nonstretched (uncompressed) ribs support):

$$
\begin{aligned}
&w_{n,j}=0,\qquad w_{n,j}=-w_{n-2,j},\qquad F_{n,j}=0,\\
&F_{n,j}=p_{x_2}+F_{n-2,j},\\
&\qquad\qquad j=1,\ldots,m-1,\\
&w_{i,m}=0,\qquad w_{i,m}=-w_{i,m-2},\qquad F_{i,m}=0,\\
&F_{i,m}=p_{x_1}+F_{i,m-2},\\
&\qquad\qquad i=1,\ldots,n-1,
\end{aligned}
\tag{8}
$$

and the following initial conditions:

$$
\begin{aligned}
w_{ij}&=f_1\left(x_{1k},x_{2k}\right),\qquad w_n'=f_2\left(x_{1k},x_{2k}\right),\\
&\qquad\qquad(0\le k\le n).
\end{aligned}
\tag{9}
$$

After reduction to the normal form, (7)–(9) are solved via the fourth-order Runge-Kutta method, where on each time step we need to solve a large system of linear algebraic equations regarding time, and a time step is yielded by the Runge principle.

## 3. Numerical Results

One of the fundamental problems of nonlinear dynamics concerns the existence of a threshold between chaotic and multimode turbulent dynamics. In this work we address this problem using a 2D continuous system as the plate, where first we illustrate numerically the scenarios of transitions from periodic to chaotic plate dynamics via period doubling bifurcations. The computed Feigenbaum constant is compared with the known value $d = 4.66916224\ldots$ (see [16]) for different choice of the partition of spatial variables while applying FDM. Values of the series $q_{0,n}$ and $d_n$ versus partition numbers (points) used in FDM are given in Table 1. Observe that an increase of the partition numbers implies an increase of DoF (degrees of freedom) of the studied system. The numerical analysis shows that the approximation to 64 DoF (number of partitions 8) is not sufficient to achieve reliable results regarding the dynamics of studied

continuous mechanical systems in the form of rectangular plates. An increase of DoF of the considered mathematical model implies the earlier illustrated occurrence of the first and successive period doubling bifurcations for the fixed amplitude of the periodic load action. The same holds for the case of chaotic dynamics. However, the obtained results are not in good agreement with the theoretically obtained Feigenbaum constant value. Applying partition number 12 we have good coincidence of the theoretical and computed Feigenbaum constant (the difference is 0.22006%), and the obtained result can be even improved through the increase of the partition number. We have used further 14 points in all computations while applying FDM.

As we have mentioned, we study regular and chaotic dynamics of a rectangular plate simply supported subjected to the periodic load action $p_{x_1} = p_{x_2} = p_0 \sin \omega_p t = p$ on the plate perimeter, where $\omega_p$ and $p_0$ are the frequency and amplitude of the external load, respectively.

Vibrations are studied in the time interval $t \in [0, 286]$, for $\lambda = a/b = 1$, dissipation factor $\varepsilon = 1$, and the Poisson coefficient $\mu = 0.3$. Results obtained for the center of the middle plate surface are generalized into the whole plate [13]. In the numerical experiment with the excitation frequency $\omega_p = 2.9$ a new modified Feigenbaum scenario has been obtained (see Table 2).

First of all it should be emphasized that already for small values of the amplitude of the excitation load with the frequency $\omega_p = 2.9$, the plate vibrates at the frequency $\omega_1 = 1.45$; that is, the first subharmonic vibration regime appears. An increase of the amplitude of the longitudinal load forces the plate to vibrate harmonically, but a further increase of this parameter provokes the occurrence of frequencies associated with the second bifurcation ($\omega_3 = 0.725$ and $\omega_2 = 2.175$), and the obtained frequencies have the power that is essentially higher than that corresponding to the frequency $\omega_p = 2.9$. When the excitation amplitude achieves 0.749, new frequency $\omega_1 = 1.45 = \omega_p/2$ appears. The power of frequencies $\omega_1$ and $\omega_p$ are commensurable but essentially lesser than the powers corresponding to frequencies $\omega_3$ and $\omega_2$. Therefore, after the third bifurcation, the plate exhibits chaotic dynamics in the whole time interval. The curves of equal deflection lose their symmetry only in the chaotic plate vibration regime.

Since we study the squared plate ($\lambda = 1$) and since the same load is applied to all plate edges, the equal deflection curves are called symmetric only if they have four axes of symmetry.

A numerical experiment, where the excitation frequency coincides with plate natural frequency ($\omega_p = \omega_0 = 5.8$), allowed us to monitor the Feigenbaum scenario to chaos different from the so far illustrated scenarios (Table 3). Here for small load amplitude we have harmonic vibrations, but its increase implies the occurrence of the next bifurcation and also an essential modification of vibration properties, which is well characterized by the 2D wavelet spectrum for $P = 0.8$. In the initial part of the studied time interval the excitation frequency dominates, whereas for $t \approx 50$ a key role plays $\omega_1 = 2.9 = \omega_p/2$. Since in this case the change of the system vibrations is realized via a narrow chaotic window, then a direct application of the classical Fourier analysis to this case is not suitable. Namely, it does not allow us to monitor peculiarities of time evolutions of the frequency characteristics of the studied vibrations.

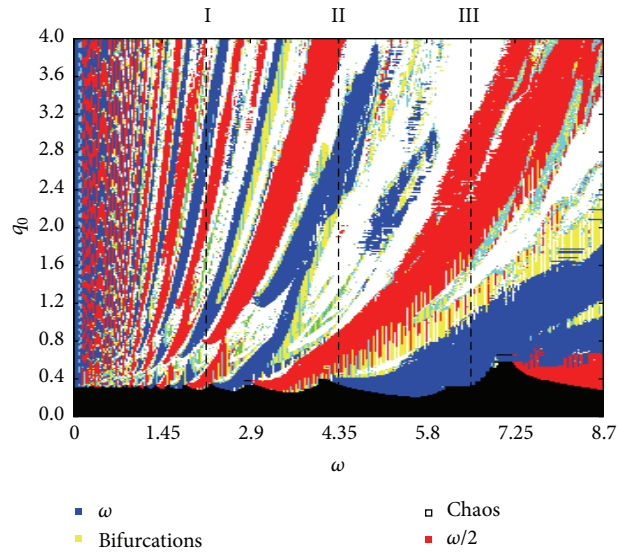


Figure 2: Chart of the character of plate vibrations.

It should be emphasized that in each of the considered time intervals we compare the obtained results with the wavelet spectrum, and the results obtained through different methods, that is, the Fourier and wavelet analyses, coincide with each other. The second bifurcation takes place for $p = 1.1$ and it appears for $t \geq 126$. A further increase of the excitation amplitude implies the occurrence of intermittency windows, which finally pulls the system into chaotic dynamics exhibited in the whole time interval. The so far described process is well illustrated via the 2D frequency wavelet spectra. Symmetry breaking of the curves of equal deflections appears only in chaotic zones.

The scenario detected via a third experiment ($\omega_p = 8.7$) begins, as in the previous case, with superiority of the first bifurcation (Table 4). Then the spectrum is periodic and an increase of the excitation frequency implies the occurrence of the first and second bifurcations. It should be emphasized that after the second bifurcation the intermittency windows occur on the wavelet spectrum, which then play a key role in the road to chaos. Another important observation is that symmetry breaking of the curves having equal deflections (isoclines) occurs already for the quasiperiodic vibrations, and the vibrations associated with the second bifurcation ($p = 2.1$) exhibit only two axes of symmetry. Chaotic plate vibrations violate in full the previous symmetry of isoclines.

We follow here a recipe given by H. Poincaré, who suggested to study instead of only one solution, a set of solutions for the chosen control parameters. Here we take the amplitude and frequency of the excitation acting on the plate perimeter as two control parameters. In order to construct a vibration type chart with the resolution $300 \times 300$, we solved and analyzed 90 000 numerical problems (Figure 2). Each of the tasks required a construction and study of time

Table 2: Applied dynamic characteristics ($\omega_p = 2.9$).

| $p_0$ $\omega_p = 2.9$ | Poincaré map $w_t(w_{t+T})$ | Fourier power spectrum $S(\omega)$ | Curves of equal deflections | 2D Morlet wavelet |
|---|---|---|---|---|
| 0.4 | 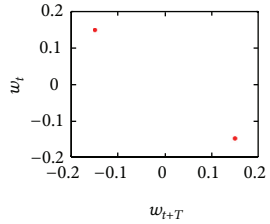 | 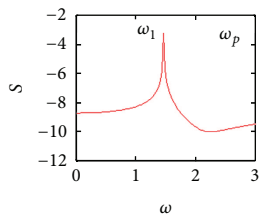 | 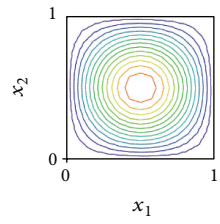 | 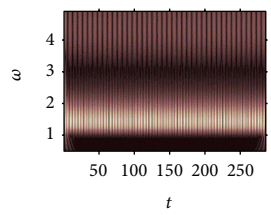 |
| **0.5** | 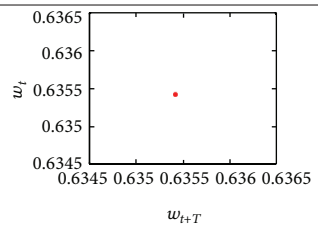 | 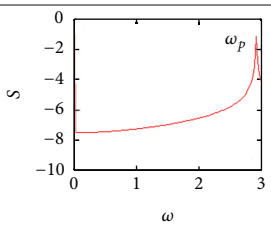 | 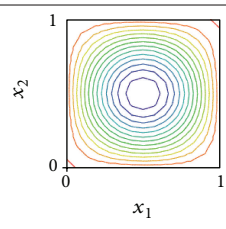 | 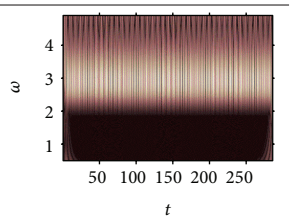 |
| 0.745 | 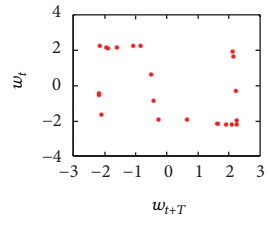 | 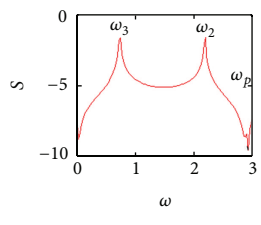 | 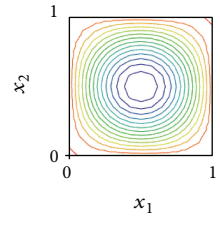 | 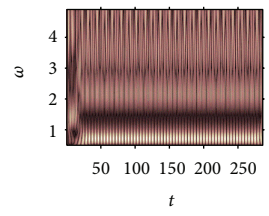 |
| 0.749 | 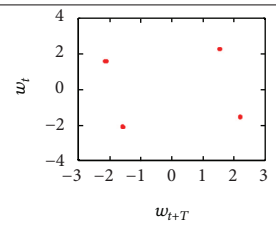 | 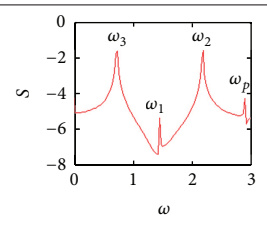 | 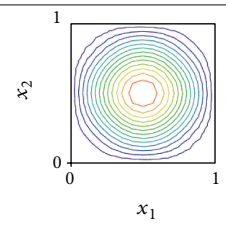 | 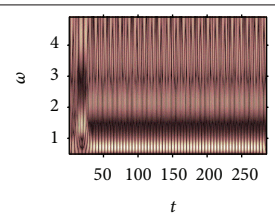 |
| 0.75 | 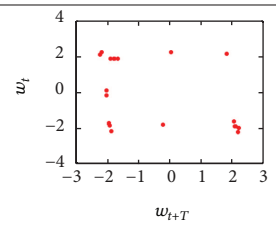 | 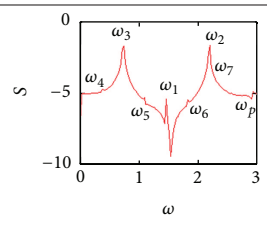 | 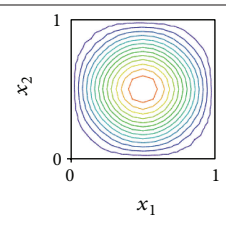 | 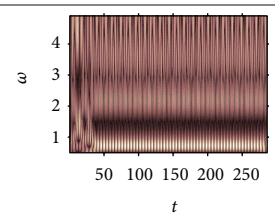 |
| 0.95 | 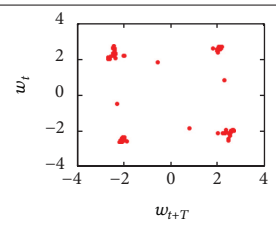 | 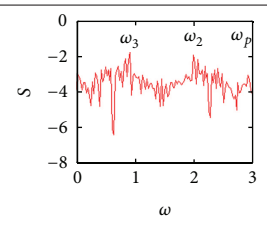 | 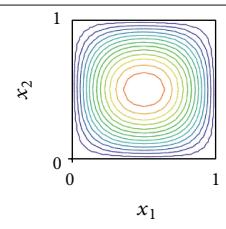 | 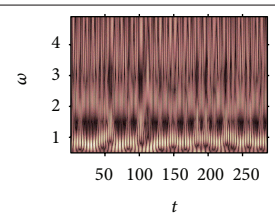 |

series (signals), phase and modal portraits, Poincaré maps, Fourier and wavelet spectra, autocorrelation functions, and the Lyapunov exponents. Owing to the results reported in the chart, for small load amplitudes, a zone of damped oscillations is observed. For small frequency values $\omega \leq 2$, narrow subharmonic zones are interlaced with narrow zones of periodic vibrations. An increase of the excitation frequency implies an increase of the area of these zones and their mixing with chaotic zones. The occurrence of a large amount of subharmonic vibrations corresponds to the physical aspect of the studied process which can be treated as the reliability and validity confirmation of the obtained numerical results.

Table 3: Applied dynamic characteristics ($\omega_p = \omega_0 = 5.8$).

| $p_0$ $\omega_p = \omega_0 = 5.8$ | Poincaré map $w_t(w_{t+T})$ | Fourier power spectrum $S(\omega)$ | Curves of equal Deflections $w(x_1, x_2)$ | 2D Morlet wavelet spectrum |
|---|---|---|---|---|
| 0.3 | 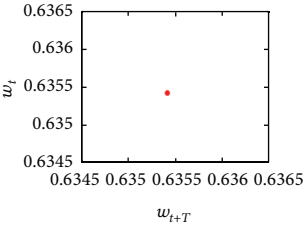 | 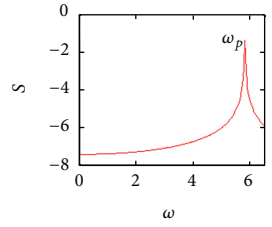 | 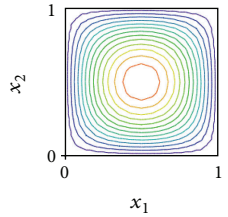 | 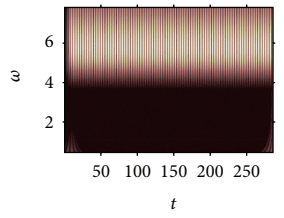 |
| 0.9 | 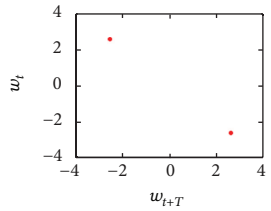 | 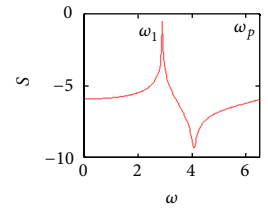 | 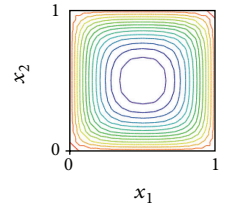 | 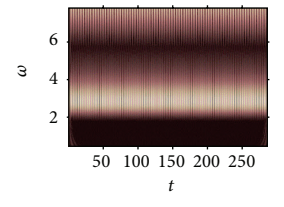 |
| 1.1 | 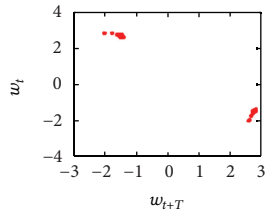 | 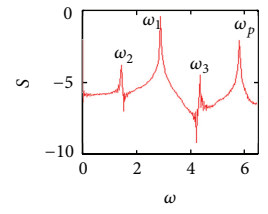 | 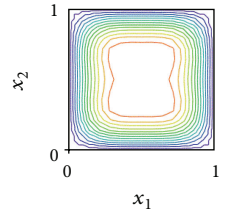 | 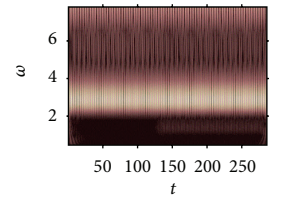 |
| | | 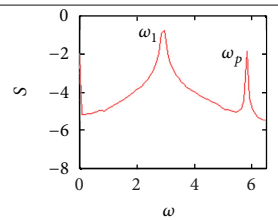 $p = 1.1,\ t \in [0, 125]$ | 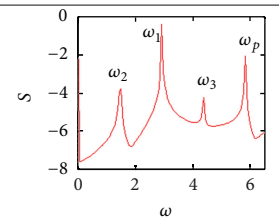 $p = 1.1, t \in [126, 286]$ | |
| 1.15 | 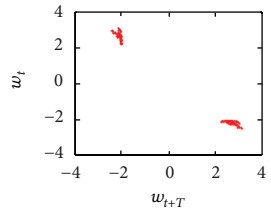 | 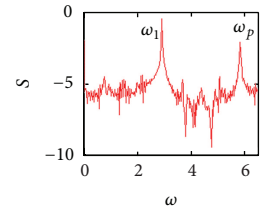 | 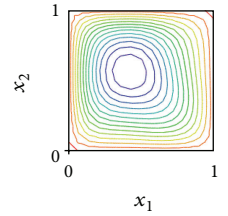 | 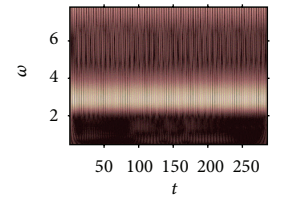 |
| 2.05 | 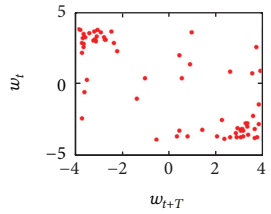 | 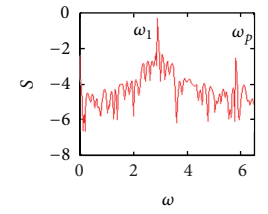 | 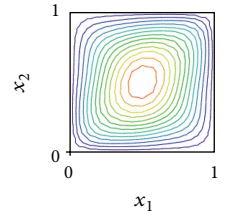 | 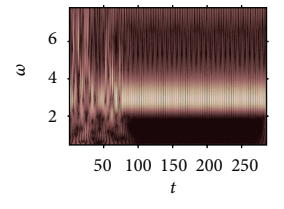 |
| 2.1 | 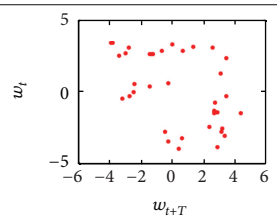 | 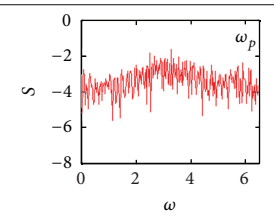 | 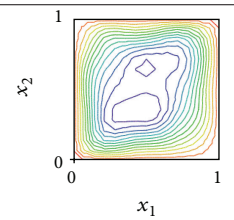 | 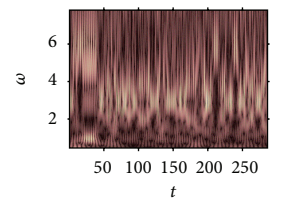 |

Table 4: Applied dynamic characteristics ($\omega_p = 8.7$).

| $p_0$ $\omega_p = 8.7$ | Poincaré map $w_t(w_{t+T})$ | Fourier power spectrum $S(\omega)$ | Curves of equal Deflections $w(x_1, x_2)$ | 2D Morlet wavelet spectrum |
|---|---|---|---|---|
| 0.3 | 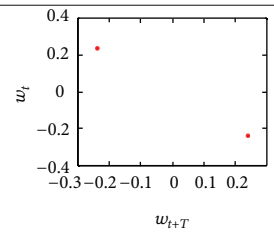 | 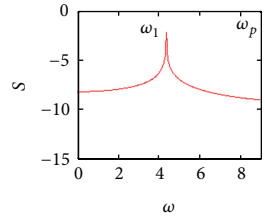 | 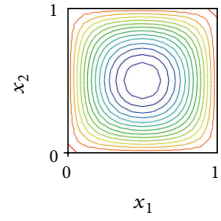 | 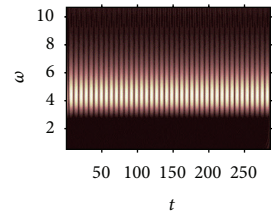 |
| 0.65 | 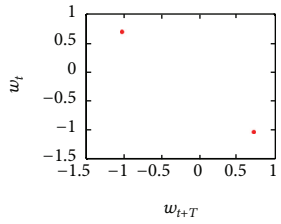 | 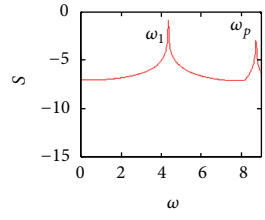 | 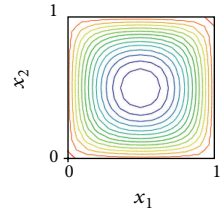 | 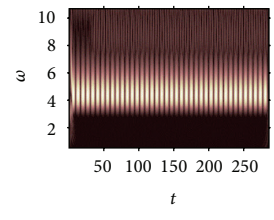 |
| 0.75 | 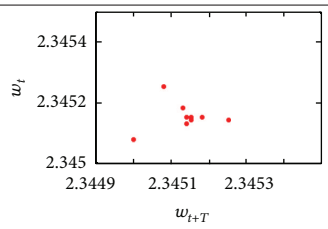 | 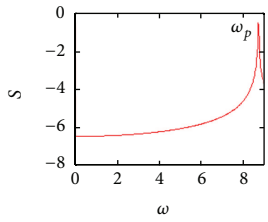 | 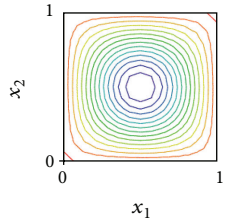 | 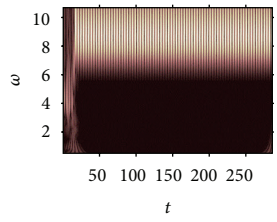 |
| 1.1 | 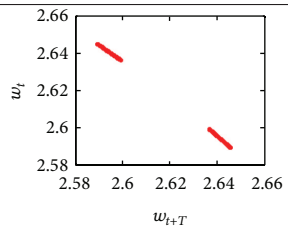 | 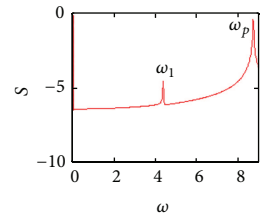 | 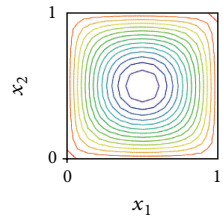 | 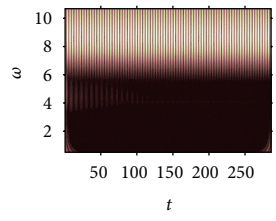 |
| 2.1 | 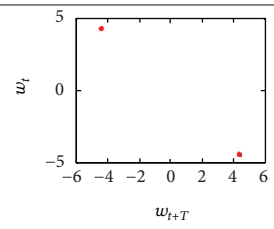 | 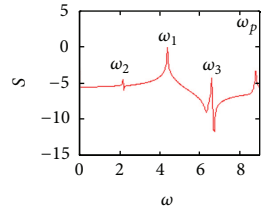 | 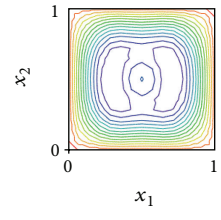 | 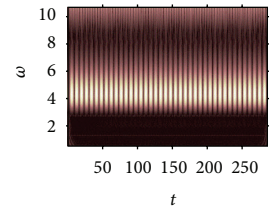 |
| 2.7 | 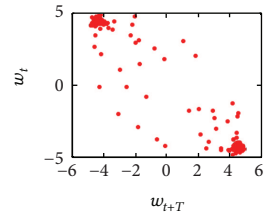 | 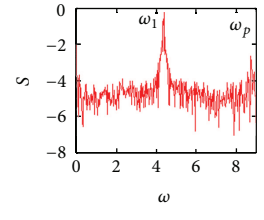 | 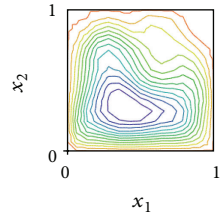 | 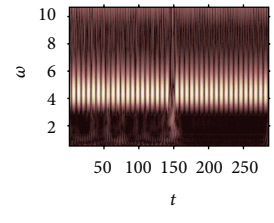 |

## 4. Concluding Remarks

In this work a simultaneous application of the Fourier and wavelet analyses allowed us to construct three different modifications of the classical Feigenbaum scenarios. It has been reported and illustrated that the plate vibration type undergoes qualitative changes not only in a standard way through the changes of the values of system parameters but also for the all fixed parameters; that is, vibrations change qualitatively when time is increased. This problem refers to estimation of the computational time unless an attractor is finally achieved. We have shown in Table 3 ($p = 1.1$) that for

simulation interval of the nondimensional time [0, 125] the Fourier spectrum exhibits only two frequencies $\omega_p$ and $\omega_1$. However, within time interval (126,286) our investigated system undergoes a second bifurcation associated with occurrence of two additional frequencies, $\omega_2$ and $\omega_3$.

It has also been shown that chaos appears already after the second Hopf bifurcation. It has been illustrated that in all studied cases the symmetry breaking of the curves of equal deflections (isoclines) occurs while transiting into a chaotic regime.

The constructed vibration chart allows us to control the dynamics of a studied continuous mechanical system. Namely, one may choose parameters of the system keeping its dynamics in a safe periodic regime. When the system dynamics is shifted into a chaotic zone, this causes loss of its stability and catastrophe.

## Conflict of Interests

The authors declare that there is no conflict of interests regarding the publication of this paper.

## Acknowledgments

This work has been supported by the National Center of Science under the Grant MAESTRO 2, no. 2012/04/A/ST8/00738 for the years 2012–2015 (Poland). J. Awrejcewicz acknowledges also a support of the Humboldt Foundation Award.

## References

[1] X. L. Yang and P. R. Sethna, "Local and global bifurcations in parametrically excited vibrations of nearly square plates," *International Journal of Non-Linear Mechanics*, vol. 26, no. 2, pp. 199–220, 1991.

[2] X. L. Yang and P. R. Sethna, "Non-linear phenomena in forced vibrations of a nearly square plate: antisymmetric case," *Journal of Sound and Vibration*, vol. 155, no. 3, pp. 413–441, 1992.

[3] T. Yamaguchi and K. Nagai, "Chaotic vibrations of a cylindrical shell-panel with an in-plane elastic-support at boundary," *Nonlinear Dynamics*, vol. 13, no. 3, pp. 259–277, 1997.

[4] A. C. J. Luo, "Chaotic motions in resonant separatrix zones of periodically forced, axially travelling, thin plates," *Proceedings of the Institution of Mechanical Engineers K: Journal of Multi-Body Dynamics*, vol. 219, no. 3, pp. 237–247, 2005.

[5] Y. Wang, "Bifurcations and chaos of bimetallic circular plates subjected to periodic heat load," *Zeitschrift für Angewandte Mathematik und Mechanik*, vol. 88, no. 4, pp. 256–266, 2008.

[6] C. Touzé, O. Thomas, and M. Amabili, "Transition to chaotic vibrations for harmonically forced perfect and imperfect circular plates," *International Journal of Non-Linear Mechanics*, vol. 46, no. 1, pp. 234–246, 2011.

[7] C. Touzé, S. Bilbao, and O. Cadot, "Transition scenario to turbulence in thin vibrating plates," *Journal of Sound and Vibration*, vol. 331, no. 2, pp. 412–433, 2012.

[8] M. Amabili, A. Sarkar, and M. P. Païdoussis, "Chaotic vibrations of circular cylindrical shells: Galerkin versus reduced-order models via the proper orthogonal decomposition method," *Journal of Sound and Vibration*, vol. 290, no. 3–5, pp. 736–762, 2006.

[9] J. Awrejcewicz, V. A. Krysko, and A. V. Krysko, "Spatio-temporal chaos and solitons exhibited by von Kármán model," *International Journal of Bifurcation and Chaos in Applied Sciences and Engineering*, vol. 12, no. 7, pp. 1465–1513, 2002.

[10] J. Awrejcewicz, V. A. Krysko, I. V. Papkova, and A. V. Krysko, "Routes to chaos in continuous mechanical systems. Part 1: mathematical models and solution methods," *Chaos, Solitons and Fractals*, vol. 45, no. 6, pp. 687–708, 2012.

[11] A. V. Krysko, J. Awrejcewicz, I. V. Papkova, and V. A. Krysko, "Routes to chaos in continuous mechanical systems. Part 2: modelling transitions from regular to chaotic dynamics," *Chaos, Solitons and Fractals*, vol. 45, no. 6, pp. 709–720, 2012.

[12] J. Awrejcewicz, A. V. Krysko, I. V. Papkova, and V. A. Krysko, "Routes to chaos in continuous mechanical systems. Part 3: the Lyapunov exponents, hyper, hyper-hyper and spatial-temporal chaos," *Chaos, Solitons and Fractals*, vol. 45, no. 6, pp. 721–736, 2012.

[13] J. Awrejcewicz, I. V. Papkova, E. U. Krylova, and V. A. Krysko, "Wavelet-based analysis of the regular and chaotic dynamics of rectangular flexible plates subjected to shear-harmonic loading," *Shock and Vibration*, vol. 19, no. 5, pp. 979–994, 2012.

[14] I. V. Andrianov, V. V. Danishevs'Kyy, and J. Awrejcewicz, "An artificial small perturbation parameter and nonlinear plate vibrations," *Journal of Sound and Vibration*, vol. 283, no. 3–5, pp. 561–571, 2005.

[15] J. Awrejcewicz, *Classical Mechanics—Dynamics*, Springer, New York, NY, USA, 2012.

[16] M. J. Feigenbaum, "Quantitative universality for a class of nonlinear transformations," *Journal of Statistical Physics*, vol. 19, no. 1, pp. 25–52, 1978.